3D RESISTIVITY IMAGING OF BURIED OIL AND TAR CONTAMINATED WASTE DEPOSITS

JONATHAN CHAMBERS[1,2], RICHARD OGILVY[1], PHILIP MELDRUM[1] and JOHAN NISSEN[3].

[1] *Fluid Processes and Waste Management Group, British Geological Survey, Keyworth, Nottingham, NG12 5GG, U.K.*

[2] *Department of Civil and Structural Engineering, The University of Sheffield, Mappin Street, Sheffield, S1 3JD, U.K.*

[3] *ABEM Instrument AB, Hamngatan 27, S-172 66 Sundbyberg, Sweden.*

(Received June 28, 1999; revised version accepted September 30, 1999)

Chambers, J, Ogilvy, R, and Meldrum, P. 1999. 3D resistivity imaging of buried oil- and tar-contaminated waste deposits. *European Journal of Environmental and Engineering Geophysics*, Vol. 4, 3-14.

ABSTRACT

Chambers, J. E., Ogilvy, R. D., Meldrum, P. I., and Nissen, J., 1999. 3D resistivity imaging of buried oil and tar contaminated waste deposits. *European Journal of Environmental and Engineering Geophysics,* 4: 3-14.

This case study illustrates the advantages of 3D resistivity surveys for mapping concealed, highly irregular tar pits containing industrial waste, mainly from oil reprocessing and coal mining. Previous geophysical surveys and intrusive sampling had confirmed the irregular geometry of the pits and the heterogeneity of the waste products but, at the time, 3D resistivity surveys were not a practical option. With recent advances it has now been possible to obtain a more accurate spatial model based on 3D resistivity datasets and full 3D inversion.

The survey was carried out using a network of individual lines within a grid measuring 95 m by 95 m. The data were modeled using a 3D inversion program (RES3DINV) and the resulting resistivity distributions were then displayed as volumetric 3D tomograms.

Three zones of low resistivity were identified as pits 4N, 4S and 1A respectively. The 3D model provided valuable diagnostic information on the geometry of the pits; the distribution and nature of in-filling waste materials and zones where leachate had infiltrated the bedrock. The results were confirmed by ground-truth derived from trial pits, cone penetration tests, historic photographs and boreholes.

KEYWORDS: resistivity tomography, 3D inversion, buried waste.

INTRODUCTION

Voids generated by clay extraction at a site in Derbyshire have been subsequently filled with a variety of waste materials including acid tars, colliery spoil and oil saturated fuller's earth. Previous geophysical surveys using EM conductivity soundings and VLF profiling clearly located the waste filled pits, but these methods were unable to accurately determine their geometry, nor the distribution and nature of the waste.

Recent developments in inversion software and electrical surveying instrumentation now allow the collection and interpretation of 3D data sets (Loke and Barker, 1996; Park, 1998; Brunner et al., 1999; Ogilvy et al., 1999). An area of the site thought to contain three waste-filled clay pits has been investigated using 3D resistivity tomography to further constrain the geometries of the pits and to estimate the nature and distribution of the waste.

SITE HISTORY AND DESCRIPTION

The site has a history of coal and clay extraction, with the removal of clay continuing up until 1980. During the 1970s, permissions were granted for the tipping of waste materials in the voids generated by the clay extraction. Materials including tar wastes, mining/quarry spoil, oil saturated bentonite and foundry sands, fuller's earth and building rubble are known to have been tipped at the site. Attempts were made to stabilise and stiffen the tar by the addition of lime and ash.

The site as a whole has very uneven topography as a consequence of mineral extraction, and contains three large lagoons. However, part of the area (Fig. 1) containing pits 1A, 4N and 4S is relatively flat. The surficial material was firm enough to allow walk-over surveys and the placement of electrodes for resistivity surveys. The site is situated on the Westphalian Coal Measures, which comprise a repetitive sequence of mudstone, siltstone, sandstone, seat earth and coal. Pits 4N, 4S and 1A were produced from the extraction of clay from the mudstone sequence containing the Lower Brampton coal seam, which is underlain by more competent sandstone. The general dip of the strata across the site is approximately 15^0 E.

PREVIOUS INVESTIGATIONS

Previous conventional site characterisation techniques included Schlumberger resistivity soundings, EM soundings (Geonics EM38, EM31 and EM34), VLF-R profiling, cone penetration tests, boreholes and trial pit excavations. An attempt was made to model the geophysical results using 1D inversion and 2D forward VLF-R modelling to derive a pseudo-3D spatial model. The pit boundaries were well defined but some discrepancies were observed between ground-truth and geophysical models at depth. The difficulties in "forcing" a 1D or 2D fit in such a heterogeneous environment were self-evident.

The combined use of conventional site investigation techniques and photographic records and maps of the site during its working life established the presence of pits 4N, 4S and 1A. However, the precise geometries of the pits were not known. Pits 4N and 4S were thought to extend to maximum depths of 9 m and 11 m

respectively, and to be separated by a narrow wall of un-excavated clay. It was estimated that pit 1A extends to a depth of 9 m, and that its base followed the surface of the underlying sandstone. Pits 1A and 4S were known to be dominated by oil-contaminated fuller's earth, with lesser amounts of ash and clinker, colliery spoil and other general fill materials. The fuller's earth is a waste product from oil re-refining activities and produces leachate with a low pH and relatively high concentrations of sulphate as a result of treatment with sulphuric acid. The composition of the fuller's earth waste varies widely across the site. Pit 4N (Fig. 2) contains a high proportion of acid tar saturated silt, which generally has a lower pH than that of the oil contaminated fuller's earth.

The previous geophysical surveys established that the acid tars and leachates had very low resistivities of below 15 Ω.m and 1 Ω.m respectively. The resistivity of the bedrock (mudstone, clay and sandstone) varied between 10 and 100 Ω.m, though in general was above 30 Ω.m. Hence the resistivity contrast between the tar, other contaminated materials and the bedrock provided a basis for mapping the waste pits. However, only a weak resistivity contrast was observed between the bedrock and other fill materials such as mining/quarry spoil and ash and clinker, making it more difficult to distinguish these features on the basis of resistivity values alone. The oil-contaminated fuller's earth has a low resistivity due to sulphate contamination.

METHOD

Instrumentation

The survey was undertaken using a prototype electrical imaging system (Fig. 3) primarily designed to map non-aqueous phase liquids such as oils, tars and solvents. The system measures both chargeability and resistivity but in the present case study only surface resistivity data are considered.

A maximum of 96 electrodes can be utilised at any given time. The instrument has four channels to reduce data collection time. A laptop computer is used to address electrodes, set current levels and measurement times, to acquire measurements, and to store data. Current settings of between 150 and 250 mA were used, with measurement windows of between 0.2 and 0.4 seconds.

Survey Design

The survey was carried out using a colinear pole-dipole electrode array. Measurements were carried out along individual lines, within a grid measuring 95 m by 95 m. Survey lines comprised a maximum of 20 stainless steel electrodes at 5 m intervals. The separation between consecutive lines was 10 m. Survey lines were placed in both the X and the Y directions to minimise the influence of strike-orientation on the final model e.g.: the easterly dipping underlying strata. A small number of electrode positions were not used due to obstructions such as ponds and mounds of rubble. These electrode positions were generally at the ends of lines. The survey lines used within the survey grid are shown in Fig. 1. The survey grid could not be extended further north due to the presence of tar contaminated surface pools and marshy ground.

In accordance with standard nomenclature the dipole spacing is referred to as ‘a’, whilst the number of ‘a’ spacings between the current electrode and the potential

dipole is referred to as ‘n’. The ‘a’ spacings used were 5 m and 10 m. The ‘n’ spacings were between 1 and 10 for an ‘a’ of 5 m, and between 1 and 7 for an ‘a’ of 10 m. The additional use of the larger 10 m ‘a’ spacing allowed a greater effective depth of investigation, as well as increasing data density. The remote electrode positions for survey lines in the X and Y directions were at 230, 870 and –545, -180 respectively, relative to the origin of the survey grid.

Numerical Inversion

The inversion of the resistivity field data was carried out using the 3D finite difference inversion program RES3DINV (Loke and Barker, 1996). The inversion program uses a block model in which resistivity values are assigned to prisms within a 3D mesh. The program attempts to achieve convergence between the observed apparent resistivity values and calculated model by using the Gauss-Newton smoothness constrained least squares method (deGroot-Hedlin and Constable, 1990, Sasaki, 1992, Loke and Barker, 1996), in which the Jacobian sensitivity matrix is recalculated after each inversion. The blocks of the first two model layers were divided in half, vertically and horizontally, in order to provide better resolution of the calculated resistivity distribution. The relative proximity of the remote electrode was accommodated in the program by using the exact geometric factor when calculating apparent resistivity values. The inversion was carried out to the point at which the difference between consecutive RMS errors was less than 5%. RMS error values of below 10% were regarded as acceptable.

A total of 6927 individual apparent resistivity measurements was made during the course of the survey. The 3D inversion of the field data resulted in a resistivity model consisting of 8305 data points prior to interpolation. A RMS error of 4.6 % was achieved after 4 iterations. The time taken to complete the 4 iterations was 22 hours on a Pentium III 450 MHz PC. The calculated resistivity model consists of a mesh measuring 95 by 95 m, extending to a depth of 34 m. The resistivity distributions associated with the presence of the waste pits fell within the upper half of the model.

3D Visualisation

An interpolated data set was generated from the 3D inverted data using an inverse distance algorithm. In this method voxel node values are assigned using the weighted average of values of the nearest points in each 90^0 sector around the node.

A 3D visualisation package was used to display the interpolated data as a combination of solid iso-resistivity surfaces and sections, or solely as a set of sections. The iso-resistivity surfaces were set to best define the geometry of the feature of interest (Table 1). Iso-resistivities were set to 15 Ω.m to delineate conductive waste, such as acid tar and sulphates, and 90 Ω.m to delineate more resistive material such as rubble fill and uncontaminated sandstone bedrock. The visualisation package is designed to be used interactively in order to view the 3D image from all conceivable directions. In this paper screen views have been selected which best show features of interest.

Table 1. Estimated and measured resistivity values of various waste materials.

Waste	Resistivity (Ohm.m)
Acid tar	< 15
Leachate	< 1
Oil contaminated fuller's earth	5 to 30
Rubble fill	> 90

Results

Fig. 4a shows relatively resistive areas (>90 Ω.m) across the surface of the site which may be attributed to inert fill materials, such as rubble, which were observed during the course of the survey. Towards the base of the model a gently dipping, relatively high resistivity layer was identified, and is thought to represent a sandstone unit known to underlie the site. Fig. 4b shows areas of low resistivity (<15 Ω.m) which were identified as areas of tar contamination and other conductive waste materials. A conductive structure was identified along the western boundary of the site, dipping gently to the north from a depth of 2 to 6 m. The structure appeared to be linear, though it may extend laterally to the west. This feature could represent a buried drainage structure or a metallic pipeline.

In some zones the true geometry of the pits may be masked by the penetration of leachate into the surrounding bedrock, so only approximate depths can be inferred using the inverted resistivity model. The similarity between the resistivity of some waste materials and the surrounding bedrock may also obscure the true geometries of the pits.

Two discrete areas of low resistivity, <15 Ω.m, were identified within the eastern area of the survey grid, and appear to correspond to pits 4N and 4S. An area of higher resistivity (35-45 Ω.m) identified in TP14A and borehole S8 as unworked clay bedrock, separates the two areas. The area of unworked clay appears to extend from Y = 15 to Y = 30 m.

Pit 4N

The survey grid covered only part of pit 4N. Previous investigations of this pit have revealed the presence of a high concentration of acid tar contaminated silts. This pit is seen in Fig. 4b as a conductive region of <15 Ω.m, extending to depths of between 12 and 17 m, with a maximum lateral extent bounded by X = 30 m and Y = 15 m. Cone penetration test C31 carried out 18 m north of the survey area identified the base of pit 4N as extending to a depth of 11 m. The greater than expected depth of pit 4N as indicated by the calculated resistivity model may be a function of poor vertical resolution, or more probably reflects infiltration by leachate into the underlying bedrock and along joint and bedding planes. Leachate infiltration occurs in other areas of the site and the high concentration of acid tar and associated leachates in pit 4N would suggest that this is the most likely explanation. The pit is capped by 2 to 3 m of more resistive (17-30 Ω.m) material, some of which was observed on site to

be weathered tarry silts. The weathering process appears to have raised the pH of the tar, thereby increasing the resistivity of the tarry silts.

Pit 4S

Pit 4S contains more resistive materials than pits 4N and 1A. The pit appears to be bounded by resistive fill to the north and south at approximately Y = 30 and 70 m respectively, and to the west at approximately X = 35 m. The base of the pit, as defined by the distribution of low resistivity values and the absence of resistivity contrast with the bedrock, appears to fall between depths of 8 and 11 m. The maximum depth of the pit as determined by intrusive sampling is 9.6 m, as indicated in borehole S09.

The heterogeneous nature of the resistivity distribution within this area indicates that a number of materials of differing resistivity are present. The records of trial pits TP15, TP16 and TP18 support this proposition, in which no less than six different materials were identified: fuller's earth, ash and clinker, mining spoil, compacted bricks and gravel. The pit is known to contain large quantities of oil contaminated fuller's earth, which due to its sulphate content, gives a low resistivity value. The patches of particularly conductive material defined by the <15 Ω.m iso-resistivity surface on Fig. 4b are therefore attributed to areas of high oil concentration. The relatively conductive acid tar is thought to be absent from this pit. Zones of high resistivity seen on Fig. 5b towards the surface of the pit are likely to represent rubble fill, as observed in trial pits TP15, TP16 and TP18.

Pit 1 A

The resistivity model of Fig. 4b indicates that the eastern wall of the pit falls between X = 44 and 48 m to the north of the survey area. The records of TP11 support this finding. The site investigation report suggested that the base of pit 1A follows the dip of the underlying sandstone bedrock, which has a general dip across the site of 15^0. The resistivity model (Fig. 5a) indicates that the base of the pit has a dip of approximately 13^0E, which corresponds closely to that of the underlying sandstone. The deepest part of the pit appears to coincide with its eastern boundary, at which point it reaches a depth of between 8 and 11 m. Trial pit TP11 and the inverted resistivity model indicate that the eastern wall of the northern sector of pit 1A is bounded by a steep wall. The resistivity model (Fig. 5a) indicates a benched floor in the northern area of the pit, and this is supported by historical records and the records of trial pits in other areas of pit 1A. Trial pit TP10 records a stepped increase in depth from west to east. The resistivity model also indicates a bench feature at this location at an identical depth.

Figs. 4 and 5a show that pit 1A contains a relatively high concentration of material with resistivities below 15 Ω.m, particularly in the area defined by X = 44 to 80 m and Y = 0 to 40 m. This resistivity distribution is consistent with the presence of oil contaminated fuller's earth. The lower resistivity values associated with this pit relative to pit 4S indicate that the fuller's earth in pit 1A contains a greater concentration of acidic oils, and associated sulphate contamination. The easterly migration of leachate from pit 1A can be seen on Fig. 5a as a zone of low resistivity

values following the dip of underlying strata. Patches of resistive material, likely to be rubble fill, overlie the eastern part of the pit.

CONCLUSIONS

The 3D resistivity imaging technique has been successful in producing a resistivity model of three waste pits that corresponds well with historical records and the findings of intrusive investigation techniques, including trial pits and cone penetration tests. The 3D resistivity images were used to interpolate between ground-truth and to further constrain the geometries of pits 4N, 4S and 1A. The dual advantages of volumetric and non-invasive surveys are particularly important where sampling by intrusive techniques (e.g. boreholes, penetrometers) may be difficult, non-representative and hazardous.

Pits 4N and 4S were shown to be separated by a narrow wall of unexcavated material, and to extend to depths of 17 m and 11 m respectively. The actual base of pit 4N is likely to be nearer 12 m, with infiltration of leachate causing the conductive feature, which persists to 17 m. The resistivity images indicate that the benched base of pit 1A follows the dip of the underlying sandstone.

Pit 4N displays a high concentration of material with a resistivity of <15 Ω.m, which correlates well with the presence of a high proportion of acid tar. Pits 1A and 4S contain a heterogeneous distribution of resistivities, and are known to contain a similar range of waste materials. Resistivities within pit 4S were generally higher than those within pit 1A, indicating that the fuller's earth in pit 1A contains a higher concentration of acidic oils and associated sulphate contamination. The calculated resistivity model has also shown that leachate from pit 1A may be migrating at depth in an easterly direction.

Unlike many other non-aqueous phase liquids, e.g. coal tars, the oils and tars within this study area were found to be electrically conductive. The results confirmed that the intrinsic electrical properties of the waste products must be known, and not assumed, if 3D resistivity models are to be used to differentiate between various in-fill materials.

ACKNOWLEDGEMENTS

The resistivity survey described in this paper was carried out using a prototype electrical imaging system developed by ABEM Instrument AB, Sweden, in partnership with the British Geological Survey and BG Technology Plc with part funding from the Commission of the European Union (Contract SMT4-CT96-2056). The authors wish to thank Ian Campbell of Scott Wilson Kirkpatrick and Co. Ltd. for arranging access permissions and providing control data. Thanks are also due to Steve Shedlock and Oliver Kuras for their assistance in the field during the course of the survey. This paper is published with the permission of the Director of the British Geological Survey, a component body of the Natural Environment Research Council.

REFERENCES

Brunner, I., Friedel, S., Jacobs, F. and Danckwardt, E. 1999. Investigation of a Tertiary maar structure using three-dimensional resistivity imaging. Geophysical Journal International, 136: 771-780.

deGroot-Hedlin, C. and Constable, S. 1990. Occam's inversion to generate smooth, two-dimensional models from magnetotelluric data. Geophysics, 55: 1613-1624.

Loke, M. H. and Barker, R. D. 1996. Practical techniques for 3D resistivity surveys and data inversion. Geophysics, 44: 499-523.

Ogilvy, R. D., Meldrum, P. I. and Chambers, J. E. 1999. Imaging of industrial waste deposits and buried quarry geometry by 3-D resistivity tomography. European Journal of Environmental and Engineering Geophysics, 3: 103-114.

Park, S. 1998. Fluid migration in the vadose zone from 3-D inversion of resistivity monitoring data. Geophysics, 63: 41-51.

Sasaki, Y. 1992. Resolution of resistivity tomography inferred from numerical simulation. Geophysical Prospecting, 40: 453-463.

FIGURES

Fig. 1. Resistivity survey lines and locations of trial pits, cone penetration tests and boreholes over pits 1A, 4N and 4S. Electrodes are situated at 5 m intervals along the survey lines.

Fig. 2. View of resistivity survey line across pit 4N.

Fig. 3. The prototype ABEM electrical imaging system.

Fig. 4. Resistivity tomogram of pits 4N, 4S and 1A. Iso-resistivity volumes opaque (a) above 90 ohm.m and (b) below 15 ohm.m.

Fig. 5. Resistivity sections in X-Z plane along (a) Y = 14 m and (b) Y = 62 m, generated from 3D resistivity survey over pits 4N, 4S and 1A.

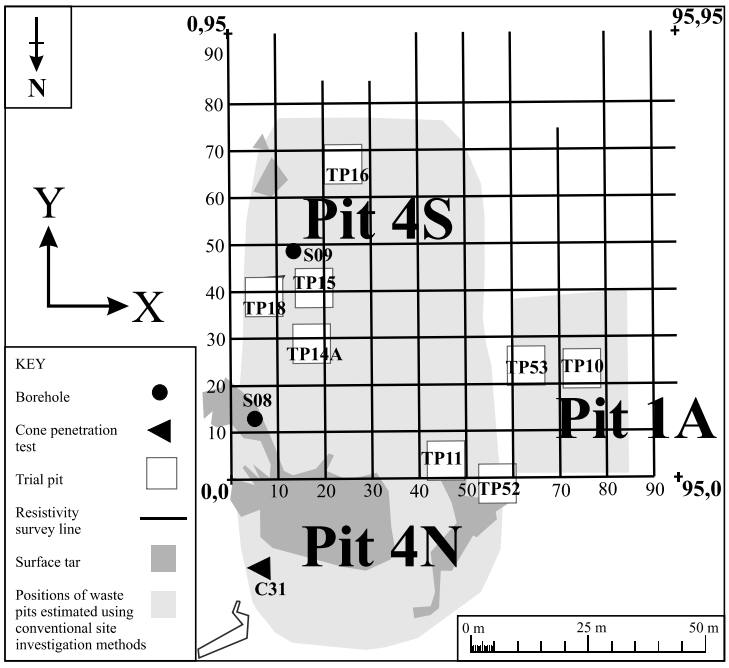

Fig. 1. Resistivity survey lines and locations of trial pits, cone penetration tests and boreholes over pits 1A, 4N and 4S. Electrodes are situated at 5 m intervals along the survey lines.

Fig. 2. View of resistivity survey line across pit 4N.

Fig. 3. The prototype ABEM electrical imaging system.

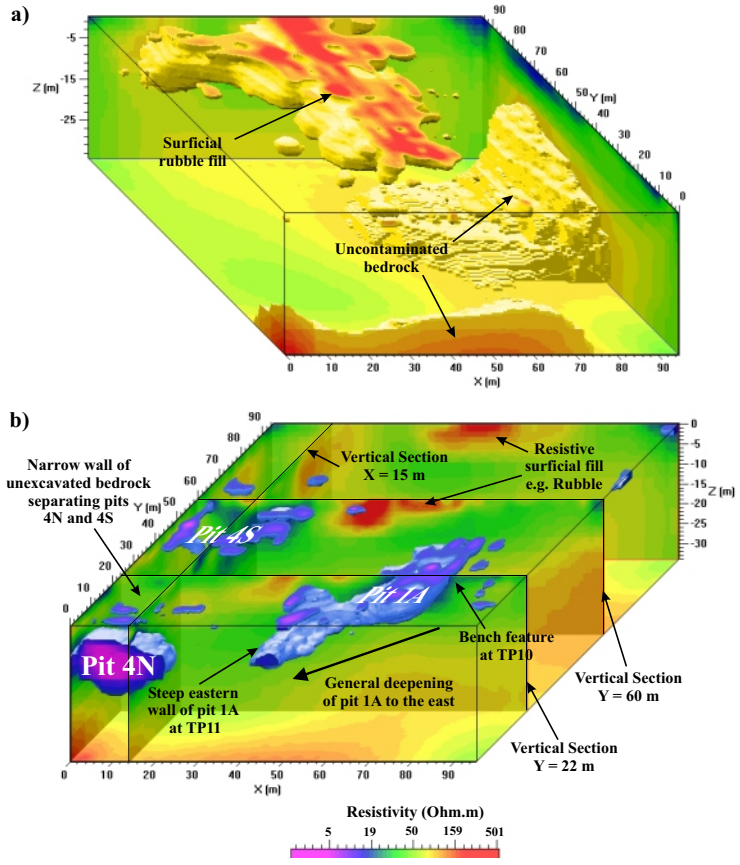

Fig. 4. Resistivity tomogram of pits 4N, 4S and 1A. Iso-resisitivity volumes opaque (a) above 90 ohm.m and (b) below 15 ohm.m.

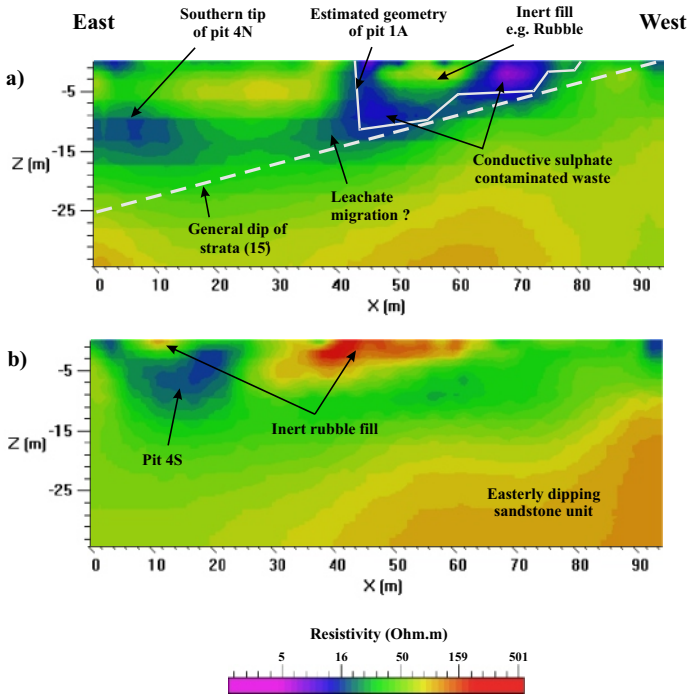

Fig. 5. Resistivity sections in X-Z plane along (a) Y = 14 m and (b) Y = 62 m, generated from 3D resistivity survey over pits 4N, 4S and 1A.